La radiologia medica
https://doi.org/10.1007/s11547-018-0955-7

ONCOLOGY IMAGING

Whole-body magnetic resonance imaging (WB-MRI) in oncology: recommendations and key uses

Giuseppe Petralia[1,2,3] · Anwar R. Padhani[4] · Paola Pricolo[1] · Fabio Zugni[5] · Marco Martinetti[3] · Paul E. Summers[1] · Luigi Grazioli[6] · Stefano Colagrande[7] · Andrea Giovagnoni[8] · Massimo Bellomi[1,2,3] · On behalf of the Italian Working Group on Magnetic Resonance

Received: 24 July 2018 / Accepted: 23 October 2018

Abstract
The past decade has witnessed a growing role and increasing use of whole-body magnetic resonance imaging (WB-MRI). Driving these successes are developments in both hardware and software that have reduced overall examination times and significantly improved MR imaging quality. In addition, radiologists and clinicians have continued to find promising new applications of this innovative imaging technique that brings together morphologic and functional characterization of tissues. In oncology, the role of WB-MRI has expanded to the point of being recommended in international guidelines for the assessment of several cancer histotypes (multiple myeloma, melanoma, prostate cancer) and cancer-prone syndromes (Li–Fraumeni and hereditary paraganglioma–pheochromocytoma syndromes). The literature shows growing use of WB-MRI for the staging and follow-up of other cancer histotypes and cancer-related syndromes (including breast cancer, lymphoma, neurofibromatosis, and von Hippel–Lindau syndromes). The main aim of this review is to examine the current scientific evidence for the use of WB-MRI in oncology.

Keywords Magnetic resonance imaging · Diffusion-weighted imaging · Oncology · Whole-body MRI · Cancer screening · Cancer-related syndromes

Introduction

In 1905, Albert Einstein published an article in *Annalen der Physik* describing the random motions of small particles suspended in a fluid that provided the first quantitative theory for the natural phenomenon widely known as the *Brownian motion*. Essentially, Einstein's theory allows one to relate the diffusion constant to physical quantities, such as the mean squared displacement of a particle in a given interval of time [1]. Denis Le Bihan published the first article displaying diffusion-weighted magnetic resonance images of the central nervous system in 1985 [2], some 80 years after Einstein's theory on water diffusion. Since then, diffusion-weighted imaging (DWI) has evolved as a clinical magnetic resonance imaging (MRI) technique; it first entered practice in neuroradiology for the assessment of cerebral ischemia [3] and subsequently has extended into oncological applications [4, 5].

In 2004, Taro Takahara started applying DWI in a single, whole-body (WB) examination, thus giving birth to the WB-MRI examination as we know it today: used mostly in oncological applications to provide a combination of morphologic

✉ Paul E. Summers
paul.summers@ieo.it

1 Department of Radiology, IEO, European Institute of Oncology IRCCS, Milan, Italy

2 Department of Oncology and Hematology, University of Milan, Milan, Italy

3 Advanced Screening Centers - ASC Italia, Castelli Calepio, Bergamo, Italy

4 Paul Strickland Scanner Centre, Mount Vernon Hospital, Northwood, UK

5 Postgraduate School in Radiodiagnostics, University of Milan, Milan, Italy

6 First Department of Radiology, Civic and University Hospital of Brescia, Brescia, Italy

7 Department of Experimental and Clinical Biomedical Sciences, Radiodiagnostic Unit n. 2, University of Florence - Azienda Ospedaliero-Universitaria Careggi, Florence, Italy

8 Department of Radiology, Ospedali Riuniti, Università Politecnica delle Marche, Ancona, Italy

Published online: 14 November 2018

and diffusion-weighted images from head to mid-thigh. Taking steps to ensure good background body suppression of the signal, this first whole-body MRI (WB-MRI) with DWI examinations took almost an hour to acquire and required off-line image concatenation to produce an unified stack of slices for visualization [6]. As highlighted in recent meta-analyses [7, 8], the growing evidence regarding the use of WB-MRI in oncology has come to support recommendations of whole-body MRI in international guidelines [9–11] and widening clinical adoption for different cancer histotypes [12, 13].

Our aim is to review the current scientific evidence for the use of WB-MRI in oncology.

Imaging acquisition protocol

The uptake of WB-MRI as a radiological technique is closely tied to technical developments that have contributed to achieving a good spatial resolution with good signal-to-noise ratio throughout the body, including continuous moving-table acquisitions, multi-channel surface receiver coils, and parallel imaging acquisition. These developments have dramatically reduced the scanning time for WB-MRI, such that DWI can now be performed along with supporting morphologic T1- and T2-weighted images of the whole body in a reasonably short acquisition time (30–45 min).

The anatomical coverage of a WB-MRI examination is usually from the skull base to mid-thigh analogous to positron emission tomography (PET) and computed tomography (CT) scans, though in specific clinical contexts it may be extended from vertex to feet. Imaging is usually performed with a large field of view (40–45 cm) [14].

Morphologic images

Due to their short acquisition times, T1-weighted images of the chest and abdomen are usually performed within breath-holds as this prevents misinterpretation due to motion artifacts. Gradient echo (GE) and Dixon techniques are increasingly used for the T1-weighted images due to their capability to derive multiple images (including in-phase, opposite phase, water, and fat images) in a single acquisition. T1-weighted imaging is usually acquired in the same plane as the DWI images to ensure a good anatomical match. Intravenous contrast agent administration with subsequent post-contrast T1 image acquisition is performed only for specific clinical requests, such as the detection of brain metastases or characterization of liver masses.

Post-processing of the Dixon images and specifically derivation of a fat fraction ($F\%$) map that describes fat distribution are recommended [15]. A fat fraction map can be computed on most of the MRI post-processing consoles as:

$$100 \times F/(F + W)$$

where F and W are, respectively, the fat and water images produced by the Dixon technique.

T2-weighted images are acquired in the axial plane without fat suppression using turbo spin-echo (TSE) sequences, with half-Fourier acquisition single-shot turbo spin-echo (HASTE) being preferred. Notably, some centers do not include T2-weighted images in the WB-MRI protocol in order to limit the acquisition time as similar information is provided by low *b*-value DWI images, but at a lower spatial resolution.

T1-weighted images and T2-weighted images with fat suppression via short tau inversion recovery (STIR), acquired the spine in the sagittal plane, are usually warranted for investigation of suspected skeletal metastasis.

Diffusion-weighted images

DWI is usually performed using relatively thick sections (from 5 to 7 mm) in an axial orientation during free breathing using a single-shot spin-echo planar imaging (SSH-EPI) acquisition, to reduce both acquisition time and image distortion. Fat suppression with the STIR is strongly recommended in order to provide homogeneous fat signal suppression at larger fields of view.

In the interest of limiting examination duration, two *b*-values are usually sufficient but three or more *b*-values are likely to more precisely quantify the apparent diffusion coefficient (ADC) value, as requested for the tumor response assessment. The lowest *b*-value is usually in the range from 50 to 100 s/mm^2 to minimize perfusion-related signal, while the highest is typically between 800 and 1000 s/mm^2 to allow good detection of hyper-cellular lesions with a good signal-to-noise ratio. Depending on the MR scanner homogeneity and patient size, between four and six stacks of contiguous slices (corresponding to different bed positions) are usually necessary to perform WB-MRI from skull base to mid-thigh.

Post-processing of the DWI data is mandatory and should consist of:

- Unification of the high *b*-value images into a single series (consecutive from superior to inferior),
- Generation of maximum intensity projections (MIPs) of the unified high *b*-value series at small angular increments (typically 3°) rotating around the cranial–caudal axis,
- Generation of coronal multi-planar reconstructions (MPRs) of the unified high *b*-value series,
- If dedicated T2-weighted images were not acquired, unify the low *b*-value images into a single series,
- Unification of the ADC maps into a single series (consecutive from superior to inferior).

MIP reconstructions are usually displayed with an inverted gray scale, to provide a panoramic view similar to PET examinations. A complete image acquisition protocol is summarized in Table 1, and a typical example of WB-MRI imaging, including DWI, is displayed in Fig. 1.

Other possible WB-MRI protocols

Other WB-MRI protocols for oncology have been used in the studies published over the last 15 years. Their differences can be described in terms of the following four concepts: anatomical coverage, imaging planes, MR sequences and reconstructions, and contrast administration.

The *anatomical coverage* can be extended from the vertex to the feet (including upper limbs) when evaluating bone involvement in diseases that frequently involve the long bones, such as multiple myeloma (MM) [16, 17], when evaluating soft tissues in melanoma patients [18, 19], as well as for cancer screening in patients with Li–Fraumeni syndrome [20]. Extending the anatomical coverage implies longer acquisition times.

As regards *imaging planes*, many studies have made use of the coronal plane for morphologic whole-body images, alone or in combination with axial imaging [16, 21–29]. In some cases, this choice may allow a better trade-off between scan time and image coverage, but is also a matter of scanner performance, radiologist preference, local practices, and considerations of readability, for example, the axial skeleton [30]. The addition of dedicated single body part imaging is worth considering for specific assessment of brain, liver [31, 32], and chest [32]. Sagittal acquisition of the whole spine is included in the majority of WB-MRI published protocols [21–25, 27, 31–34], as it allows rapid acquisition and efficient evaluation of vertebral lesions, spinal cord compression, and vertebral fractures [26].

The choice of the *MR sequences and reconstructions* used in WB-MRI protocols has seen considerable evolution, and while not all include DWI [21–25, 32], the majority of studies without DWI were published between 2002 and 2013, when DWI of the whole body was quite time-consuming and quality inconsistent. MR technology developments in the last few years have significantly improved the quality and time efficiency of DWI in large volumes, allowing its wider and easier application in WB-MRI protocols. Similarly, the use of *F%* maps that we suggest in this review for bone assessment is a recent introduction to WB-MRI and is only described in two studies published in 2017, using WB-MRI for multiple myeloma [17] and breast cancer [34, 35] patients. That earlier studies did not make use of *F%* maps is probably due to progressive acceleration of the Dixon acquisition and prior lack of experience with this application in WB-MRI.

Contrast administration is reported primarily in studies where WB-MRI was used for patients with tumors requiring brain assessment, such as melanoma [18, 31] and lung adenocarcinoma [27]. The administration of contrast is also described in several studies including patients with MM. However, DWI has largely replaced the administration of contrast agents in many studies performed in patients with osteotropic tumor histotypes [26, 34–36] and lymphoma [29, 37].

Clinical applications in oncology

Multiple myeloma

Multiple myeloma (MM) is a hematological disorder characterized by the accumulation of neoplastic plasma cells in the bone marrow. The resulting bone disease is characterized by the presence of osteolytic lesions, osteoporosis, or bone fractures and has a significant impact on morbidity and mortality

Table 1 WB-MRI acquisition protocol: morphologic and diffusion-weighted imaging

Images	Sequences	Image contrast	Fat suppression	Plane	Acquisition mode	Reconstructions
Morphologic	GE	T1	Dixon	Axial	Breath hold	*F%*
	HASTE	T2	\			
	TSE	T1	\	Sagittal	Free breathing	\
		T2	STIR			
DWI	SSE SE EPI	low b-value 50–100 s/mm^2 high b-value 800–1000 s/mm^2	STIR	Axial	Free breathing	Unification of the high *b*-value images into a single series MIPs of the unified high *b*-value series rotating around the cranial–caudal axis Coronal MPRs of the unified high *b*-value series Unification of the ADC maps into a single series


a
T1 (DIXON) in phase
T1 (DIXON) opposite phase
T1 (DIXON) water image
T1 (DIXON) fat image
T2 HASTE
F%
T1
T2 STIR
b
b 50
b 900
ADC
MIP

◂**Fig. 1** **a** Morphologic images acquired during WB-MRI examination. The anatomical coverage is from the skull base to mid-thigh. Axial scans include multiple T1-weighted images from a single Dixon acquisition (namely in-phase, out of phase, water, and fat images) and T2- weighted images performed without fat suppression. The *F*% map is computed from the T1-weighted Dixon image data. Sagittal T1- and T2-weighted (with STIR fat suppression) images are useful for the investigation of metastases in the spine. **b** Diffusion-weighted images acquired as part of a WB-MRI examination. The anatomical coverage is from the skull base to mid-thigh. Two different diffusion weightings (with *b*-values of 50 s/mm^2 and 900 s/mm^2, respectively, in this example) are used to calculate the ADC map (third column). Maximum intensity projections of the high *b*-value images are used to perform rotational reconstructions, here displayed in frontal projection

in multiple myeloma patients. For this reason, the International Myeloma Working Group (IMWG) has affirmed that even the presence of asymptomatic bone disease on conventional radiography should be considered a criterion of symptomatic MM, requiring treatment [38]. In a study conducted by Walker et al. involving 611 MM patients, WB-MRI detected more focal lesions than conventional whole-body x-rays in three of the most common metastatic sites for MM, including spine (78% versus 16%; *p* value 0.001), pelvis (64% versus 28%; *p* value 0.001), and sternum (24% versus 3%; *p* value 0.001) [39]. Similar results were observed in a prospective cohort study conducted by Baur–Melnyk on 41 newly diagnosed MM patients, in which WB-MRI showed diagnostic performance superior to conventional whole-body computed tomography (CT) in the detection of skeletal lesions (CT understaged 11/41 patients compared to MRI, $p < 0.001$) [40]. In consideration of emerging evidence, the IMWG and the British Society for Haematology (BSH) have both recommended WB-MRI for the staging of all forms of multiple myeloma (Grade A recommendation, GR A [41]), as well as for the follow-up of oligo-secretory and nonsecretory myelomas (Level of Evidence LE 1B) or for patients with extramedullary diseases (LE 1B) [10, 38, 41]. Finally, WB-MRI is also recommended for the staging of solitary bone plasmacytoma (SBP), an early-stage malignancy with a clinical course between monoclonal gammopathy of undetermined significance (MGUS) and MM [38].

Melanoma

Although newly discovered immunological treatments for advanced melanoma have significantly increased overall survival, most patients with stage III–IV melanoma will still die of the disease [42]. Therefore, the clinical management of these patients requires frequent monitoring with a technique having good diagnostic performance in assessment of the entire body. In a prospective study conducted by Muller-Horvat et al. involving 41 metastatic melanoma patients, WB-MRI performed with contrast agent administration but without DWI detected some 40% more lesions than whole-body CT. Moreover, treatment strategy was altered due to the WB-MRI findings in 10 (24%) of the patients [43]. In a later study involving 71 scans, WB-MRI with DWI but without contrast-enhanced scans and WB-DWI without DWI but with contrast agent were seen to have an equivalent diagnostic performance in the detection of extracranial metastases from advanced melanoma [31]. Thus, there is growing evidence of the value of WB-MRI with DWI in both the detection and the staging of advanced melanoma, as illustrated in the cases depicted in Figs. 2 and 3.

Based on these results, the German Dermatological Society (GDS), the Dermatologic Cooperative Oncology Group (DCOG), and the recently updated Swiss guidelines recommend WB-MRI for cross-sectional imaging of advanced melanoma (stage III or worse), indicating the equivalence of this method to whole-body CT and PET/CT. Moreover, WB-MRI is recommended for the follow-up of melanoma patients staged from IIC to IV [9, 44].

Prostate cancer

Mortality rates for prostate cancer are low, despite it being the most common cancer among males in Europe [45]. This is tied to the fact that most prostate cancer diagnoses are made while the disease is still in an early stage, and thus of low–intermediate risk. There exists, however, a subgroup of prostate cancer patients who can be considered to be of high risk because their clinical parameters (prostate serum antigen (PSA) > 20 ng/mL or > cT2c or with a Gleason score GS ≥ 8) are associated with a greater probability of developing locoregional or metastatic lesions [46].

For the staging of high-risk prostate cancer patients, guidelines developed by the European Association of Urology (EAU) recommend at least cross-sectional abdominopelvic imaging and a bone scan (BS) (GR A, LE 2A) [11]. They acknowledge, however, that WB-MRI is the most sensitive imaging technique, citing a meta-analysis by Shen et al. [47] including 1102 metastatic prostate cancer patients, in which WB-MRI was found to be more sensitive (97%) than choline PET/CT (91%) and BS (78%) in the detection of skeletal metastasis (Fig. 4).

In metastatic castration-resistant prostate cancer (mCRPC) patients treated with enzalutamide, abiraterone, or radium-223, up to one disease progression in three is detected radiologically in the absence of clinical symptoms or PSA progression [15]. Furthermore, prostate-specific membrane antigen (PSMA) PET/CT scans may fail to provide information on tumor viability during androgen receptor inhibition [48]. A recent review conducted by Padhani et al. [49] indicates the potential of WB-MRI to address unmet clinical needs in mCRPC patients. Similarly, the European Organization for Research and Treatment of

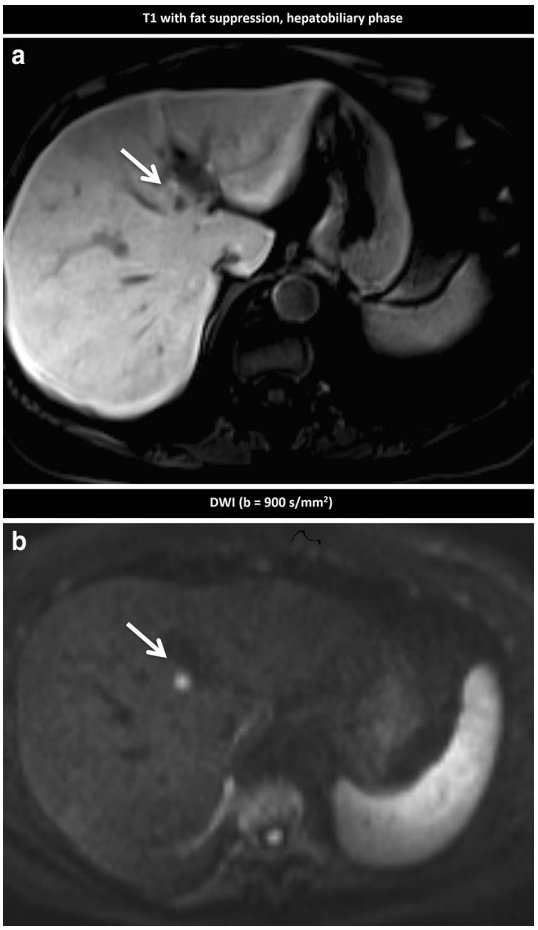

Fig. 2 Contrast-enhanced (gadolinium-ethoxybenzyl-diethylenetriamine pentaacetic acid, Gd-EOB-DTPA) WB-MRI with DWI performed on a patient with a stage III melanoma. Hepatobiliary phase 20 min after injection (**a**) reveals the presence of a 9 mm metastasis in the fourth liver segment (white arrow). The same lesion is clearly detectable in the high *b*-value (900 s/mm^2) diffusion-weighted image performed in the same session (**b**)

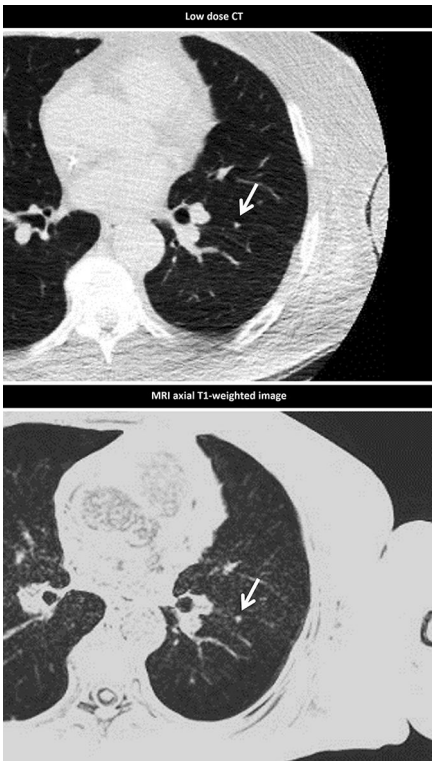

Fig. 3 Follow-up evaluation of a patient with stage IV melanoma using low-dose CT of the lung and WB-MRI. A subcentimetric metastasis in the left inferior lobe of the lung is detected on the axial CT image (arrow in **a**) as well as axial T1-weighted image (arrow in **b**)

Cancer (EORTC) considers WB-MRI as a "one-size-fit-all" solution for evaluating treatment efficacy in advanced prostate cancer patients [50].

The Advanced Prostate Cancer Consensus Conference (APCCC) has confirmed that PSA alone is not reliable for monitoring disease activity in mCRPC, suggesting the use of a robust imaging technique before deciding to start a new line of treatment. In this respect, their guidelines recognize the superior diagnostic performance of WB-MRI relative to CT and BS in the detection and assessment of skeletal metastasis [51], though they note limited availability of the WB-MRI technique.

Lymphoma

Fluorodeoxyglucose (FDG)-PET/CT is the imaging technique recommended for the most common lymphomas, including diffuse large B cell lymphoma (DLBCL), follicular, and Hodgkin subtypes, all of which are usually characterized by a high glucose metabolism and thus likely to be FDG-avid histotypes [52]. Consistent with this, the National Comprehensive Cancer Network (NCCN) recommends serial CT or PET/CT examinations for both the staging and follow-up of lymphoma patients [53]. In lymphoma subtypes that exhibit variable FDG avidity or non-FDG avidity however, FDG-PET/CT may be ineffective. The sensitivity of WB-MRI with DWI to hyper-cellular lesions, independent of glucose metabolism, allows a reliable radiological evaluation of these lymphoma subtypes [54].

In a prospective study conducted by Mayerhoefer et al. [13] on 140 patients, WB-MRI with DWI demonstrated better sensitivity (94.4%) than FDG-PET/CT (60.9%) and contrast-enhanced CT (70.7%) in staging patients with lymphoma subtypes of variable FDG avidity. (The majority were MALT lymphomas.) Further, the same group found WB-MRI with DWI to have a diagnostic performance similar to FDG-PET/CT and CT in FDG-avid lymphomas [55].

A growing application of WB-MRI in lymphoma involves young patients irrespective of histotype. In a

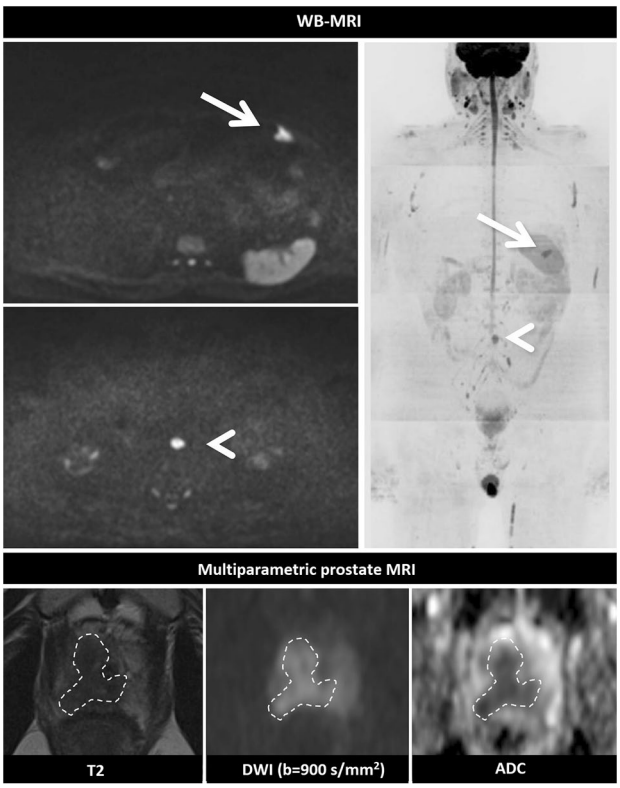

Fig. 4 A patient admitted with an initial diagnosis of prostate adenocarcinoma (GS 5+4, biopsy positive in 8/8 cores), PSA = 29 ng/mL, positive digital rectal examination (cT2c). The systemic staging, previously assessed with contrast-enhanced CT examinations of chest, abdomen, and pelvis (CT-CAP) and BS, was negative for metastatic disease. Subsequent systemic staging with WB-MRI with DWI showed two metastases, one in the anterior arch of a left rib (arrow) and the other at level of retroperitoneal lymph node (arrowhead). A multiparametric MRI examination performed in the same session showed a PI-RADS five lesion (dashed line), visible on T2-weighted axial images, high *b*-value diffusion-weighted images, and ADC map

recent study by Brenner et al., the overall 10-year survival for lymphoma patients younger than 35 years of age was seen to be above 90% (94.7% for patients < 24 years and 89.4% for patients comprised between 25 and 35 years, respectively) [56]. Despite this long survival, the NCCN guidelines still recommend PET/CT or CT for the staging and follow-up of lymphoma patients [57], with 6–9 examinations to be performed in the first two years after diagnosis. This is particularly high exposure to ionizing radiation for young patients with a long life expectancy. In justifying the choice of imaging technique, one should consider the growing evidence of equivalent diagnostic performance of WB-MRI in respect of PET scans for both staging and follow-up of lymphoma patients [13, 58–65] (Fig. 5). As summarized in Table 2, the kappa coefficient of agreement observed between these two imaging techniques is typically in the range from 0.68 to 1.00.

Breast Cancer

In the last two decades, conservative treatments and early detection have substantially improved the prognosis for patients with low-stage breast cancer (BC) [66]. Nevertheless, according to the American Cancer Society, 5-year overall survival for patients with advanced (stage IV) BC remains unfavorably low at just 22% [67]. A recent epidemiological study by Kwast et al. including 25,336 women with newly diagnosed BC demonstrated bone to be the most common site of metastatic spread, regardless of tumor histological characterization. Notably, bone metastases were present at the first staging procedure in 49.7% of invasive ductal cancer (IDC) and in 61.7% of invasive lobular cancer (ILC) subtypes, respectively [68]. The widely accepted Response Evaluation Criteria in Solid Tumors (RECIST) are not suited to a proper assessment of bone metastases and in fact consider them to not be measurable. Even the revised RECIST 1.1 version does not fully address the need to assess bone metastases. According to the new criteria, bone metastases are considered measurable only once they have spread to the surrounding soft tissue with an extent larger than 10 mm in diameter, which rarely occurs in clinical practice [69]. This situation points to a significant unmet clinical need for means to evaluate bony metastases, with implications beyond breast cancer.

In a 2011 meta-analysis by Yang et al. [70] covering 145 studies with 15,221 metastatic cancer patients, WB-MRI showed diagnostic performance comparable to PET and superior to CT and BS in the detection of skeletal metastases (Table 3). In addition, two recent studies emphasize the potential of WB-MRI in advanced breast cancer. Comparing the findings of 210 paired WB-MRI and CT-CAP for the follow-up of metastatic BC patients, Kosmin et al. observed that out of the 46 treatment changes made due to progressive disease (PD) detected at imaging, in 34.7% of the cases (16 paired examinations), PD was visible only on WB-MRI and not on the CT-CAP examinations [12]. Similarly among 40 cases of progressive disease findings in a group of 58 patients who had both WB-MRI and CT-CAP or an ^{18}F-FDG-PET/CT within 8 weeks, Zugni et al. [71] found that all 40 (100%) have been identified on WB-MRI but only 23 (58%) were also identified by CT-CAP or ^{18}F-FDG-PET/CT.

WB-MRI has also shown promising diagnostic performance and established itself as a safe and accurate diagnostic imaging method for the systemic staging of pregnant BC patients; some 40% of whom receive a diagnosis when BC is already at an advanced stage [72]. In this setting, accurate systemic staging of disease using imaging techniques that avoid ionizing radiation and contrast agent administration is to be preferred (Fig. 6).

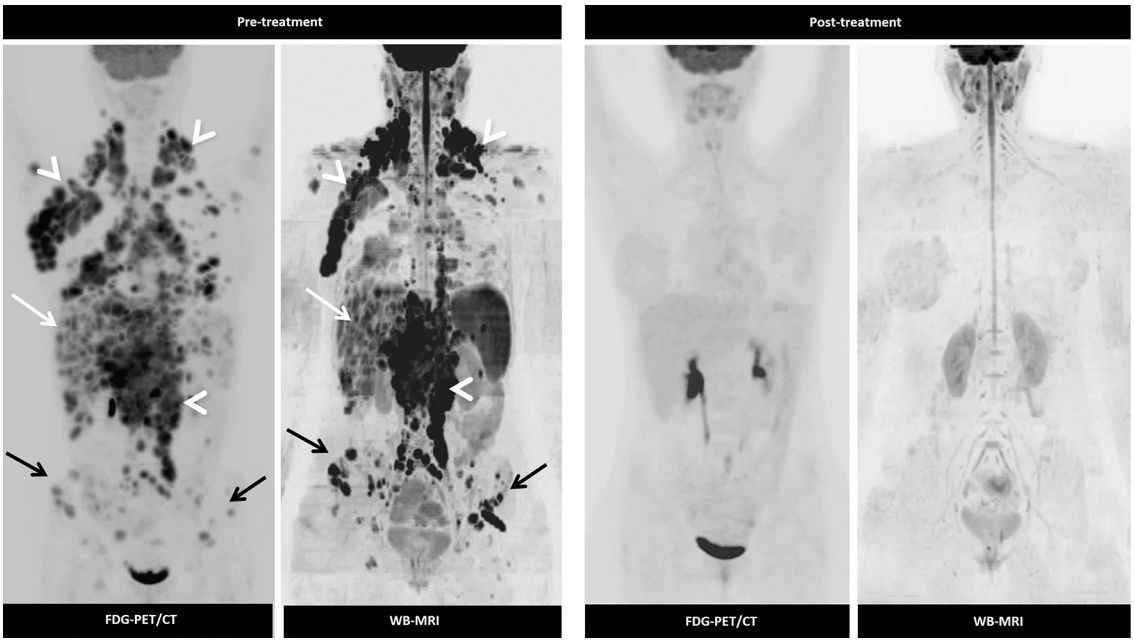

Fig. 5 A 22-year-old woman with relapse of non-Hodgkin lymphoma (Ann Arbor stage IVb). After multiple lines of systemic treatments FDG-PET/CT and WB-MRI were performed before and 6 months after initiating chemotherapy under the ESHAP scheme and peripheral blood stem cell transplantation. Response assessment with both PET/CT and WB-MRI at the same time points reveals a complete resolution of the abnormal FDG uptake across all body regions, consistent with complete response (CR)

Table 2 Level of agreement observed between WB-MRI and PET/CT techniques for staging not-FDG avid and variable FDG avidity lymphoma subtypes

References	*N*	Lymphoma histotypes	Kappa coefficient	Agreement	*P* value
Mayerhoefer et al. [13]	140	FDG-avid/non-FDG-avid lymphomas	0.92/0.89	Excellent	< 0.0001
Albano et al. [58]	104	HL, NHL	0.93	Excellent	< 0.01
Albano et al. [59]	68	HL, NHL	0.88	Excellent	< 0.05
Abdulqadr et al. [60]	31	HL, aggressive NHL, indolent NHL	0.87	Excellent	< 0.0001
Stèphane et al. [61]	23	HL, DLBCL, NHL	1.00	Excellent	< 0.0001
Van Ufford et al. [62]	22	HL, NHL	0.68	Good	< 0.0001
Gu et al. [63]	17	HL, NHL	0.82	Excellent	< 0.0001
Lin et al. [64]	15	DLBCL	0.85	Excellent	< 0.0001
Wu et al. [65]	8	DLBCL	1.00	Excellent	< 0.0001

N = number of patients, Kappa coefficient was considered corresponding to the following levels of agreement < 0 = no agreement, 0–0.20 = poor agreement, 0.21–0.40 = fair agreement, 0.41–0.60 = moderate agreement, 0.61–0.80 = good agreement, and 0.81–1.00 = excellent agreement

Finally, in the last decade the use of WB-MRI has seen progressive growth in the management of BC patients having an ILC subtype [35]. ILC is statistically more likely than IDC to spread to the gastrointestinal organs, the peritoneum and retroperitoneum, the gynecological system, and the pleura (ILC 20% and IDC 8.4%, respectively) [68], which are notoriously challenging body regions to explore using PET/CT and CT techniques. This may in part be because ILC typically follows a pattern of diffuse infiltration characterized by "Indian file" neoplastic growth related to a reduced (or absent) E-cadherin membrane expression that reduces cell-to-cell adhesion and facilitates permeation along tissue planes [73]. Further, metastases from ILC are less FDG-avid than other BC histotypes and therefore less visible on FDG-PET examinations. Due to the aspecific nature of diffusion-weighted images (hypercellular lesions are always visible at high *b*-values, regardless of the glucose metabolism), WB-MRI with DWI has the capability to depict the presence of neoplastic spread into gastrointestinal organs (Fig. 7).

Table 3 Comparison of diagnostic performances (sensitivity and specificity) between WB-MRI, CT, PET, and BS in the detection of bone metastases (based on the meta-analysis in [70])

	WB-MRI (%)	CT (%)	PET (%)	BS (%)
Per-patient analysis				
Sensitivity	90.6	72.9	89.7	86.0
Specificity	95.4	94.8	96.8	81.4
Per-lesion analysis				
Sensitivity	90.4	77.1	86.9	75.1
Specificity	96.0	83.2	97.0	93.6

Values reported on a per-patient and per-lesion analysis, respectively

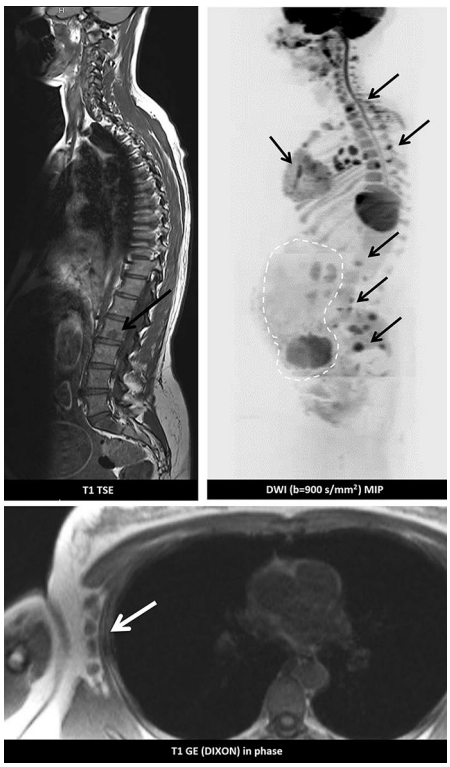

Fig. 6 WB-MRI for the systemic staging of disease in a 37-year-old woman with locally advanced BC (cT2N1) at 31 weeks of gestation. Multiple skeletal metastases (arrows) in spine, sternum, and pelvis are visible on both morphologic (T1-weighted sagittal TSE) and high *b*-value diffusion-weighted images (MIP). Several pathological lymph nodes are visible in the right axillary region on T1-weighted gradient-echo Dixon in-phase image (white arrow). High-intensity regions visible in the abdomen (dashed line) on high *b*-value diffusion-weighted images correspond to the fetal kidneys and brain. Based on the WB-MRI examination, the patient underwent an early cesarean delivery and was subsequently treated with both chemotherapy and hormonal therapy. The child did not experience adverse events during the prenatal or development periods

Other cancer histotypes

In the last few years, several articles have clearly demonstrated WB-MRI to have excellent diagnostic performance in staging and monitoring of other cancer histotypes. Lung cancer, for example, is usually staged by PET/CT together with dedicated brain MRI examinations, but in a prospective study conducted by Usuda et al. including 81 non-small cell lung cancer (NSCLC) patients, WB-MRI with DWI achieved a diagnostic performance similar to PET/CT and brain MRI in pre-surgical staging. Moreover, they found WB-MRI to provide higher diagnostic accuracy (87.6% 71/81) than PET/CT (82.7% 67/81) for the staging of hilar and mediastinal lymph nodes (N) [74]. Similar results emerged from a study by Ohno et al. involving 96 postoperative NSCLC patients that compared WB-MRI with DWI to PET/CT in the assessment of local recurrence and distant metastases. Here, WB-MRI with DWI exhibited lower sensitivity (88.2%) than PET/CT (100%), but superior specificity (100% and 81%, respectively) in the assessment of regional and distant metastases in NSCLC patients [75].

WB-MRI with DWI has also proven effective for the staging and preoperative assessment of ovarian cancer. In a prospective cohort study by Michielsen et al. that included 161 patients suspected of having ovarian cancer, WB-MRI with DWI showed a significantly superior diagnostic accuracy (93%) compared to CT (82%) for determining the malignant nature of the ovarian mass. Furthermore, WB-MRI with DWI was superior to CT in the detection of cancers having non-ovarian origin (WB-MRI + DWI = 26/32 81%, CT = 10/32 31%, p value = 0.001) and to assigning the correct FIGO stage to ovarian cancers (WB-MRI + DWI = 82/94 87%, CT = 33/94 35%) [76].

Another promising result has emerged from a study conducted by Gorelik et al. [77] on 33 myxoid liposarcoma (MLS) patients, in whom WB-MRI depicted extrapulmonary metastases from MLS that were not visible at CT in 79% of the cases (7/9 metastatic patients).

Cancer screening

The excellent diagnostic performance of WB-MRI in tumor detection (overall sensitivity 90%) with low false-positive and false-negative rates is manifested in a number of meta-analyses (Table 4) [7, 8, 47]. This, together with the shortening of examination times achieved thanks to modern acquisition protocols and hardware, has extended its application to cancer screening programs. Several articles have demonstrated the potential of WB-MRI in the early detection of cancer in subjects with Li–Fraumeni syndrome (LFS), a highly penetrant, cancer-prone syndrome, caused by germline mutations of the TP53 gene that predispose carriers to

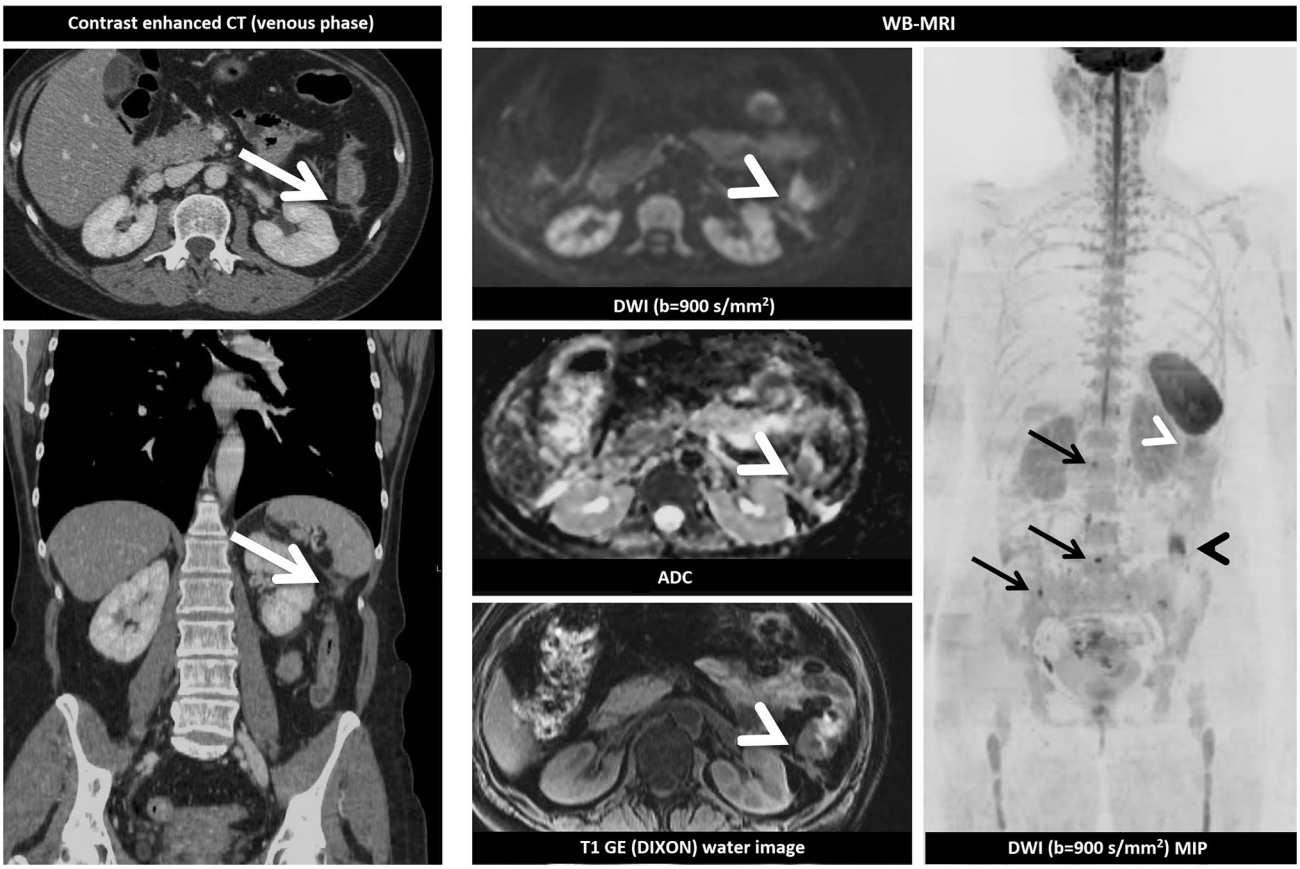

Fig. 7 In a 51-year-old metastatic ILC BC patient, tumor marker progression (CA 15-3 = 660 U/mL) occurred during third-line chemotherapy treatment. Contrast-enhanced CT of chest and lung for suspected disease progression showed the absence of secondary lesions. A thickening of the lateroconal and left anterior renal fascia (white arrow) was described as stable compared to the previous controls and interpreted as the result of a previous surgical intervention for ovarian serous cystadenoma. A suspicious thickening of the left anterior renal fascia and the descending colon wall was visible WB-MRI examination performed within a few days of the CT: the colon finding is recognizable on high *b*-value diffusion-weighted images (axial and MIP images), ADC map, and morphologic in-phase T1-weighted gradient-echo Dixon images (white arrowheads). MIP images of the high *b*-value images showed further metastatic lesions in descending colon (black arrowhead) and subcentimetric skeletal metastasis in the spine and pelvis (black arrows). All findings were confirmed at the following WB-MRI examinations

Table 4 Principal meta-analyses comparing the diagnostic performances of WB-MRI with PET in the assessment of primary and metastatic disease

References	Year	Histotype	*N*	Imaging technique	SE (%)	SP (%)
Liu et al. [7]	2017	Vertebral metastases (all cancers)	571	WB-MRI	94	94
				PET	90	63
Li et al. [8]	2014	Primary and metastases (all cancers)	1067	WB-MRI + DWI	90	95
				PET	89	97
Shen et al. [47]	2014	Bone metastases (prostate cancer)	1102	WB-MRI	95	96
				PET	87	97

N number of patients, *SE* sensitivity, *SP* specificity

a variety of cancers, including sarcoma, BC, adrenal gland carcinoma, and leukemia [78]. Around 50% of individuals with LFS will develop cancer before reaching 30 years of age, and the prevalence of LFS-related cancer rises to 95% in female subjects older than 60 years [79]. In a study by Bojadzieva et al. [80] including 63 TP53 mutation carriers, WB-MRI with contrast agent disclosed the presence of six asymptomatic tumors and one recurrent metastatic cancer, resulting in a cancer rate of 13.2%. Similar observations were found in the preliminary results from the UK SIGNIFY study, involving 44 TP53 germline mutation carriers, where WB-MRI detected the presence of four cancers that would

Table 5 Main studies of WB-MRI for cancer screening in asymptomatic individuals, sorted by number of enrolled subjects

References	Subjects	Positive for cancer	Cancer rate (%)
Ballinger et al. [20]	578	39	6.7
Mai et al. [78]	116	5	4.3
Villani et al. [82]	59	15	25.4
Bojadzieva et al. [79]	53	7	13.2
Saya et al. [80]	44	4	9,1
Anupindi et al. [83]	24	1	4.2

Cancer rate is computed as the percentage of subjects with at least one suspected or diagnosed malignancy out of the enrolled subjects

be life-threatening if left untreated, in 5 LFS subjects (cancer rate of 9.1%) [81]. A meta-analysis recently published has validated the first statistically robust estimate of the clinical utility of WB-MRI in screening TP53 mutation carriers [20]. Table 5 summarizes the main results from available cohort studies including WB-MRI examination for cancer screening in subjects with TP53 mutations [20, 79–81, 83, 84].

On the basis of the above evidence, the NCCN and the American Association for Cancer Research (AACR) have recently included annual WB-MRI examination (along with contrast-enhanced brain MRI and breast MRI for women) in their recommendations for cancer screening of individuals with LFS [85, 86].

Similarly, WB-MRI is now recommended for the baseline surveillance of subjects with hereditary paraganglioma–pheochromocytoma syndromes (HPP), genetic disorders that manifest with rare and usually benign tumors that originate in the nervous system. Aside from paragangliomas and pheochromocytomas, subjects with HPP syndromes can also develop cancers characterized by aggressive behavior, including renal cell carcinoma (RCC), gastrointestinal stromal tumors (GIST), and other rare tumor types [87]. AACR guidelines recommend biennial screening with WB-MRI for the early detection of cancer onset in subjects with HPP older than 6/8 years of age [88]. Guidelines including WB-MRI for cancer screening in genetically predisposed subjects are also under development by the Response Evaluation in Neurofibromatosis and Schwannomatosis International Collaboration (REiNS) group for early detection of cancer in neurofibromatosis (NF)-related disorders [89].

Lastly, WB-MRI is starting to see use in cancer screening in those with von Hippel–Lindau syndrome (VHL), a rare autosomal dominant disorder caused by germline mutations of human chromosome 3p25 [90]. Although MRI examinations of different body regions are already included in many institutional screening protocols for VHL subjects, no formal consensus exists as to the screening technique of choice for this rare genetic disease.

Table 6 Main studies of WB-MRI for cancer screening in LFS subjects, sorted by number of enrolled subjects

References	Subjects	Positive for cancer	Cancer rate
Bamberg (GNC) et al. [96]	30,000	Ongoing	Ongoing
Hegenscheid et al. [90]	2500	62*	2.48%
Cieszanowski et al. [95]	666	7	1.05%
Goehde et al. [91]	298	1[a]	0.33%
Lo et al. [94]	132	2	1.5%
Ulus et al. [92]	118	2	1.7%
Tarnoki et al. [93]	22	1	4.5%

Cancer rate is computed as the percentage of subjects with at least one suspected or diagnosed malignancy out of the enrolled subjects

[a]Histological confirmation not available in all subjects, GNC = German National Cohort

In the last decade, the application of WB-MRI to the early detect of cancer in asymptomatic subjects has been the subject of a number of articles (Table 6) [91–97]. The first, by Lo et al. [95], included 132 doctors from the Hong Kong Sanatorium and Hospital who underwent unenhanced WB-MRI without DWI revealed two cancers (one bronchoalveolar carcinoma and one RCC) in two (1.5%) of the participants. Similar results were observed by Cieszanowski et al. who, in a retrospective study of WB-MRI without contrast agent administration that included 666 asymptomatic individuals, found 9 malignant or possibly malignant cancers in 7 individual, corresponding to a cancer rate of 1.05% [96].

The growing interest in the potential of WB-MRI for cancer screening in asymptomatic subjects has led to its inclusion in some large cohort studies, including the German National Cohort (GNC) and UK Biobank. The German Ministry for Education and Research and other local research institutions initiated the GNC in 2015 with the aim of establishing one of the world's largest imaging data repositories, with a target of obtaining some 30,000 WB-MRI in asymptomatic subjects [97]. Similarly, the UK Biobank, a research project promoted by numerous public and private British research institutions, seeks to create the largest collection of WB-MRI scans along with a range of clinical data with the purpose of promoting the study of a wide range of diseases, including cancer, in the general population [98].

Pitfalls and limits of WB-MRI

The combined analysis of both morphologic and functional MR images is aimed at overcoming the limitations related to analysis of a single image type in whole-body MRI examinations, especially in patients with bone marrow involvement [99].

There are a number of possible sources of false-positive and false-negative findings when reviewing DWI images alone. False-positive findings in the bone marrow may be related to hemangiomas, focal areas of red bone marrow, bone marrow edema, and hyperplasia [100]. False-positive findings in soft tissues may be related to small signal abnormalities attributable to slow fluid motion in vessels, ganglia, or inflammatory processes such as inflammatory bowel disease or abscesses [101]. Importantly, the appearance of healthy lymph nodes can overlap with that of pathologic lymph nodes. The combined analysis of DWI with ADC maps and morphologic T1 and T2 images is, therefore, strongly recommended [101].

False-negative findings in bone marrow may be related to minimal disease infiltration or to the invisibility of hyperintense lesions within bone marrow hyperplasia [102] in young patients or during bone marrow stimulating treatment; in some cases, this limitation can be overcome by combined review of morphologic T1 images and *F*% maps. False-negative findings in soft tissues may occur within organs that physiologically present impeded diffusion, such as the central nervous system, salivary glands, spleen, and lymph nodes [5, 101]. Furthermore, it should be kept in mind that high signal intensity due to impeded diffusion might be suppressed in tumor histotypes characterized by mucinous or cystic structure [101]. Other false-negative findings in DWI may be related to imaging artifacts, including ghosting, poor fat suppression or magnetic susceptibility effects, that are most common in the neck, lungs, mediastinum, and left liver lobe [101]. As well, lesions in the skull might not be visible due to proximity of the brain [100].

Some pitfalls in image interpretation have been described in the assessment of response to therapy in patients with bone metastases [103]. When bone metastases respond to cytotoxic treatments or to radiation therapy, for example, an increase in bone marrow water content related to massive cell death can be observed, resulting in diffuse signal intensity reduction in T1 images. This finding might be wrongly attributed to disease progression (termed "T1-pseudoprogression") when not correlated with the appearance of bone metastases in DWI and ADC maps. Similarly, successfully treated bone metastases might show increased signal intensity in high b-value DWI images, despite showing a marked increase in ADC values; this pattern is known as "T2 shine-through" and can be recognized by combined review of DWI and corresponding ADC maps. Finally, bone metastases may show reduced signal intensity in high *b*-value images while maintaining stable ADC values; a finding associated with sclerotic evolution of the metastases, representing either progression (sclerotic progression) or response (sclerotic response) of the disease. This combination of observations should be regarded as indeterminate and requires the radiologist to carefully review morphologic T1 weighted or *F*% images, in order to correctly recognize the underlying pattern.

Conclusion

A number of oncological applications for WB-MRI are already well established and supported by clinical evidence. This evidence has led to guidelines that clearly indicate the central role of WB-MRI with DWI in the clinical management of several cancer histotypes and highlight its potential in regard to others. The lack of radiation exposure and the absence of contrast agent administration in a typical WB-MRI examination with DWI, together with good diagnostic performance, contribute to its attractiveness in application for cancer screening in both cancer-prone syndromes and asymptomatic subjects. Further work is needed to standardize acquisition protocols and interpretation practices, in order to reduce the variation in diagnostic performance. Some initial effort in this direction has been reported [15], but large-scale studies are required.

Compliance with ethical standards

Conflict of interest Summers is part owner of Company QMRI Tech, which offers consulting services in MRI. Author Summers receives consulting fees from Company ASC, Italia. All other authors declare to have no conflict of interest.

Ethical approval This article does not contain any studies with human participants or animals performed by any of the authors.

References

1. Einstein A (1905) Über die von der molekularkinetischen Theorie der Wärme geforderte Bewegung von in ruhenden Flüssigkeiten suspendierten Teilchen. Ann Phys 322:549–560. https://doi.org/10.1002/andp.19053220806
2. Le Bihan D, Breton E (1985) Imagerie de diffusion in vivo par résonance magnétique nucléaire. C R Acad Sci 93:27–34
3. Warach S, Dashe JF, Edelman RR (1996) Clinical outcome in ischemic stroke predicted by early diffusion-weighted and perfusion magnetic resonance imaging: a preliminary analysis. J Cereb Blood Flow Metab 16:53–59. https://doi.org/10.1097/00004647-199601000-00006
4. Koh D-M, Collins DJ (2007) Diffusion-weighted MRI in the body: applications and challenges in oncology. Am J Roentgenol 188:1622–1635. https://doi.org/10.2214/ajr.06.1403
5. Thoeny HC, De Keyzer F (2007) Extracranial applications of diffusion-weighted magnetic resonance imaging. Eur Radiol 17:1385–1393. https://doi.org/10.1007/s00330-006-0547-0
6. Takahara T, Imai Y, Yamashita T et al (2004) Diffusion weighted whole body imaging with background body signal suppression (DWIBS): technical improvement using free breathing, STIR and high resolution 3D display. Radiat Med 22:275–282
7. Liu T, Wang S, Liu H et al (2016) Detection of vertebral metastases: a meta-analysis comparing MRI, CT, PET, BS and BS

with SPECT. J Cancer Res Clin Oncol 143:457–465. https://doi.org/10.1007/s00432-016-2288-z
8. Li B, Li Q, Nie W, Liu S (2014) Diagnostic value of whole-body diffusion-weighted magnetic resonance imaging for detection of primary and metastatic malignancies: A meta-analysis. Eur J Radiol 83:338–344. https://doi.org/10.1016/j.ejrad.2013.11.017
9. Pflugfelder A, Kochs C, Blum A et al (2013) Malignant melanoma S3-guideline "diagnosis, therapy and follow-up of melanoma". J Dtsch Dermatol Ges. 11:1–116. https://doi.org/10.1111/ddg.12113_suppl
10. Chantry A, Kazmi M, Barrington S et al (2017) Guidelines for the use of imaging in the management of patients with myeloma. Br J Haematol 178:380–393. https://doi.org/10.1111/bjh.14827
11. Mottet N, Bellmunt J, Bolla M et al (2017) EAU-ESTRO-SIOG guidelines on prostate cancer. Part 1: screening, diagnosis, and local treatment with curative intent. Eur Urol 71:618–629. https://doi.org/10.1016/j.eururo.2016.08.003
12. Kosmin M, Makris A, Joshi PV et al (2017) The addition of whole-body magnetic resonance imaging to body computerised tomography alters treatment decisions in patients with metastatic breast cancer. Eur J Cancer 77:109–116. https://doi.org/10.1016/j.ejca.2017.03.001
13. Mayerhoefer ME, Karanikas G, Kletter K et al (2014) Evaluation of diffusion-weighted MRI for pretherapeutic assessment and staging of lymphoma: results of a prospective study in 140 patients. Clin Cancer Res 20:2984–2993. https://doi.org/10.1158/1078-0432.CCR-13-3355
14. Padhani AR, Liu G, Mu-Koh D et al (2009) Diffusion-weighted magnetic resonance imaging as a cancer biomarker: consensus and recommendations. Neoplasia 11:102–125. https://doi.org/10.1593/neo.81328
15. Padhani AR, Lecouvet FE, Tunariu N et al (2017) Metastasis reporting and data system for prostate cancer: practical guidelines for acquisition, interpretation, and reporting of whole-body magnetic resonance imaging-based evaluations of multiorgan involvement in advanced prostate cancer. Eur Urol 71:81–92. https://doi.org/10.1016/J.EURURO.2016.05.033
16. Squillaci E, Bolacchi F, Altobelli S et al (2015) Pre-treatment staging of multiple myeloma patients: comparison of whole-body diffusion weighted imaging with whole-body T1-weighted contrast-enhanced imaging. Acta Radiol 56:733–738. https://doi.org/10.1177/0284185114538792
17. Latifoltojar A, Hall-Craggs M, Bainbridge A et al (2017) Whole-body MRI quantitative biomarkers are associated significantly with treatment response in patients with newly diagnosed symptomatic multiple myeloma following bortezomib induction. Eur Radiol 27:5325–5336. https://doi.org/10.1007/s00330-017-4907-8
18. Jouvet JC, Thomas L, Thomson V et al (2014) Whole-body MRI with diffusion-weighted sequences compared with 18 FDG PET-CT, CT and superficial lymph node ultrasonography in the staging of advanced cutaneous melanoma: a prospective study. J Eur Acad Dermatol Venereol 28:176–185. https://doi.org/10.1111/jdv.12078
19. Mosavi F, Ullenhag G, Ahlström H (2013) Whole-body MRI including diffusion-weighted imaging compared to CT for staging of malignant melanoma. Ups J Med Sci 118:91–97. https://doi.org/10.3109/03009734.2013.778375
20. Ballinger ML, Best A, Mai PL et al (2017) Baseline surveillance in Li–Fraumeni syndrome using whole-body magnetic resonance imaging: a meta-analysis. JAMA Oncol 3:1634–1639. https://doi.org/10.1001/jamaoncol.2017.1968
21. Dutoit JC, Vanderkerken MA, Verstraete KL (2013) Value of whole body MRI and dynamic contrast enhanced MRI in the diagnosis, follow-up and evaluation of disease activity and extent in multiple myeloma. Eur J Radiol 82:1444–1452. https://doi.org/10.1016/j.ejrad.2013.04.012
22. Lin C, Luciani A, Belhadj K et al (2009) Patients with plasma cell disorders examined at whole-body dynamic contrast-enhanced MR imaging: initial experience. Radiology 250:905–915. https://doi.org/10.1148/radiol.2503081017
23. Lin C, Luciani A, Belhadj K et al (2010) Multiple myeloma treatment response assessment with whole-body dynamic contrast-enhanced MR imaging. Radiology 254:521–531. https://doi.org/10.1148/radiol.09090629
24. Hillengass J, Fechtner K, Weber M-A et al (2010) Prognostic significance of focal lesions in whole-body magnetic resonance imaging in patients with asymptomatic multiple myeloma. J Clin Oncol 28:1606–1610. https://doi.org/10.1200/JCO.2009.25.5356
25. Lauenstein TC, Freudenberg LS, Goehde SC et al (2002) Whole-body MRI using a rolling table platform for the detection of bone metastases. Eur Radiol 12:2091–2099. https://doi.org/10.1007/s00330-002-1344-z
26. Nakanishi K, Kobayashi M, Nakaguchi K et al (2007) Whole-body MRI for detecting metastatic bone tumor: diagnostic value of diffusion-weighted images. Magn Reson Med Sci 6:147–155. https://doi.org/10.2463/mrms.6.147
27. Takenaka D, Ohno Y, Matsumoto K et al (2009) Detection of bone metastases in non-small cell lung cancer patients: Comparison of whole-body diffusion-weighted imaging (DWI), whole-body MR imaging without and with DWI, whole-body FDG-PET/CT, and bone scintigraphy. J Magn Reson Imaging 30:298–308. https://doi.org/10.1002/jmri.21858
28. Jambor I, Kuisma A, Ramadan S et al (2016) Prospective evaluation of planar bone scintigraphy, SPECT, SPECT/CT, ^{18}F-NaF PET/CT and whole body 1.5 T MRI, including DWI, for the detection of bone metastases in high risk breast and prostate cancer patients: SKELETA clinical trial. Acta Oncol (Madr) 55:59–67. https://doi.org/10.3109/0284186X.2015.1027411
29. Adams HJA, Kwee TC, Vermoolen MA et al (2013) Whole-body MRI for the detection of bone marrow involvement in lymphoma: prospective study in 116 patients and comparison with FDG-PET. Eur Radiol 23:2271–2278. https://doi.org/10.1007/s00330-013-2835-9
30. Lecouvet FE (2016) Whole-body MR imaging: musculoskeletal applications. Radiology 279:345–365. https://doi.org/10.1148/radiol.2016142084
31. Petralia G, Padhani A, Summers P et al (2013) Whole-body diffusion-weighted imaging: is it all we need for detecting metastases in melanoma patients? Eur Radiol 23:3466–3476. https://doi.org/10.1007/s00330-013-2968-x
32. Schmidt GP, Baur-Melnyk A, Herzog P et al (2005) High-resolution whole-body magnetic resonance image tumor staging with the use of parallel imaging versus dual-modality positron emission tomography-computed tomography: experience on a 32-channel system. Invest Radiol 40:743–753
33. Hillengass J, Bäuerle T, Bartl R et al (2011) Diffusion-weighted imaging for non-invasive and quantitative monitoring of bone marrow infiltration in patients with monoclonal plasma cell disease: a comparative study with histology. Br J Haematol 153:721–728. https://doi.org/10.1111/j.1365-2141.2011.08658.x
34. Kosmin M, Makris A, Joshi PV et al (2017) The addition of whole-body magnetic resonance imaging to body computerised tomography alters treatment decisions in patients with metastatic breast cancer ScienceDirect. Eur J Cancer 77:109–116. https://doi.org/10.1016/j.ejca.2017.03.001
35. Zugni F, Ruju F, Pricolo P et al (2018) The added value of whole-body magnetic resonance imaging in the management of patients with advanced breast cancer. PLoS One. https://doi.org/10.1371/journal.pone.0205251

36. Jacobs MA, Macura KJ, Zaheer A et al (2018) Multiparametric whole-body MRI with diffusion-weighted imaging and ADC mapping for the identification of visceral and osseous metastases from solid tumors. Acad Radiol. https://doi.org/10.1016/j.acra.2018.02.010
37. Wang D, Huo Y, Chen S et al (2018) Whole-body MRI versus 18F-FDG PET/CT for pretherapeutic assessment and staging of lymphoma: a meta-analysis. Onco Targets Ther 11:3597–3608. https://doi.org/10.2147/OTT.S148189
38. Dimopoulos MA, Hillengass J, Usmani S et al (2015) Role of magnetic resonance imaging in the management of patients with multiple myeloma: a consensus statement. J Clin Oncol 33:657–664. https://doi.org/10.1200/JCO.2014.57.9961
39. Walker R, Barlogie B, Haessler J et al (2007) Magnetic resonance imaging in multiple myeloma: diagnostic and clinical implications. J Clin Oncol 25:1121–1128. https://doi.org/10.1200/JCO.2006.08.5803
40. Baur-Melnyk A, Buhmann S, Becker C et al (2008) Whole-body MRI versus whole-body MDCT for staging of multiple myeloma. Am J Roentgenol 190:1097–1104. https://doi.org/10.2214/AJR.07.2635
41. Oxford Centre for Evidence-based Medicine (2009) Levels of evidence (March 2009). https://www.cebm.net/2009/06/oxford-centre-evidence-based-medicine-levels-evidence-march-2009/. Accessed 7 July 2018
42. Hodi FS, O'Day SJ, McDermott DF et al (2010) Improved survival with Ipilimumab in patients with metastatic melanoma. N Engl J Med 363:711–723. https://doi.org/10.1056/NEJMoa1003466
43. Müller-Horvat C, Radny P, Eigentler TK et al (2006) Prospective comparison of the impact on treatment decisions of whole-body magnetic resonance imaging and computed tomography in patients with metastatic malignant melanoma. Eur J Cancer 42:342–350. https://doi.org/10.1016/j.ejca.2005.10.008
44. Dummer R, Siano M, Hunger RE et al (2016) The updated Swiss guidelines 2016 for the treatment and follow-up of cutaneous melanoma. Swiss Med Wkly. https://doi.org/10.4414/smw.2016.14279
45. International Agency for Research on Cancer (2018) IARC research topics on prostate cancer. https://www.iarc.fr/en/cancertopics/prostatetopics.php. Accessed 7 July 2018
46. Chang AJ, Autio KA, Roach M et al (2014) High-risk prostate cancer-classification and therapy. Nat Rev Clin Oncol 11:308–323. https://doi.org/10.1038/nrclinonc.2014.68
47. Shen G, Deng H, Hu S, Jia Z (2014) Comparison of choline-PET/CT, MRI, SPECT, and bone scintigraphy in the diagnosis of bone metastases in patients with prostate cancer: a meta-analysis. Skelet Radiol 43:1503–1513. https://doi.org/10.1007/s00256-014-1903-9
48. Meller B, Bremmer F, Sahlmann CO et al (2015) Alterations in androgen deprivation enhanced prostate-specific membrane antigen (PSMA) expression in prostate cancer cells as a target for diagnostics and therapy. EJNMMI Res. https://doi.org/10.1186/s13550-015-0145-8
49. Padhani AR, Lecouvet FE, Tunariu N et al (2017) Rationale for modernising imaging in advanced prostate cancer. Eur Urol Focus 3:223–239. https://doi.org/10.1016/j.euf.2016.06.018
50. Lecouvet FE, Talbot JN, Messiou C et al (2014) Monitoring the response of bone metastases to treatment with Magnetic Resonance Imaging and nuclear medicine techniques: a review and position statement by the European Organisation for Research and Treatment of Cancer imaging group. Eur J Cancer 50:2519–2531. https://doi.org/10.1016/j.ejca.2014.07.002
51. Gillessen S, Attard G, Beer TM et al (2018) Management of patients with advanced prostate cancer: the report of the advanced prostate cancer consensus conference APCCC 2017. Eur Urol 73:178–211
52. Barrington SF, Mikhaeel NG, Kostakoglu L et al (2014) Role of imaging in the staging and response assessment of lymphoma: consensus of the international conference on malignant lymphomas imaging working group. J Clin Oncol 32:3048–3058. https://doi.org/10.1200/jco.2013.53.5229
53. Hoppe RT, Advani RH, Ai WZ et al (2012) Hodgkin Lymphoma, Version 2.2012 featured updates to the NCCN guidelines. J Natl Compr Cancer Netw 10:589–597. https://doi.org/10.6004/jnccn.2012.0061
54. Ahmad Sarji S (2006) Physiological uptake in FDG PET simulating disease. Biomed Imaging Interv J 2:e59. https://doi.org/10.2349/biij.2.4.e59
55. Mayerhoefer ME, Karanikas G, Kletter K et al (2015) Evaluation of diffusion-weighted magnetic resonance imaging for follow-up and treatment response assessment of lymphoma: results of an 18F-FDG-PET/CT-controlled prospective study in 64 patients. Clin Cancer Res 21:2506–2513. https://doi.org/10.1158/1078-0432.ccr-14-2454
56. Brenner H, Gondos A, Pulte D (2009) Survival expectations of patients diagnosed with Hodgkin's lymphoma in 2006–2010. Oncologist 14:806–813. https://doi.org/10.1634/theoncologist.2008-0285
57. National Comprehesive Cancer Network (2018) NCCN clinical practice guidelines in oncology (NCCN Guidelines®) Hodgkin Lymphoma Ver. 3. https://www.nccn.org/professionals/physician_gls/default.aspx#hodgkin. Accessed 7 July 2018
58. Albano D, Patti C, Lagalla R et al (2016) Whole-body MRI, FDG-PET/CT, and bone marrow biopsy, for the assessment of bone marrow involvement in patients with newly diagnosed lymphoma. J Magn Reson Imaging 45:1082–1089. https://doi.org/10.1002/jmri.25439
59. Albano D, Patti C, La Grutta L et al (2016) Comparison between whole-body MRI with diffusion-weighted imaging and PET/CT in staging newly diagnosed FDG-avid lymphomas. Eur J Radiol 85:313–318. https://doi.org/10.1016/j.ejrad.2015.12.006
60. Abdulqadhr G, Molin D, Åström G et al (2011) Whole-body diffusion-weighted imaging compared with FDG-PET/CT in staging of lymphoma patients. Acta Radiol 52:173–180. https://doi.org/10.1258/ar.2010.100246
61. Stéphane V, Samuel B, Vincent D et al (2013) Comparison of PET-CT and magnetic resonance diffusion weighted imaging with body suppression (DWIBS) for initial staging of malignant lymphomas. Eur J Radiol 82:2011–2017. https://doi.org/10.1016/j.ejrad.2013.05.042
62. Quarles Van Ufford HME, Kwee TC, Beek FJ et al (2011) Newly diagnosed lymphoma: initial results with whole-body T1-weighted, STIR, and diffusion-weighted MRI compared with 18F-FDG PET/CT. Am J Roentgenol 196:662–669. https://doi.org/10.2214/AJR.10.4743
63. Gu J, Chan T, Zhang J et al (2011) Whole-body diffusion-weighted imaging: the added value to whole-body MRI at initial diagnosis of lymphoma. Am J Roentgenol 197:W384–W391. https://doi.org/10.2214/ajr.10.5692
64. Lin C, Itti E, Luciani A et al (2011) Whole-body diffusion-weighted imaging with apparent diffusion coefficient mapping for treatment response assessment in patients with diffuse large B-cell lymphoma: pilot study. Invest Radiol 46:341–349. https://doi.org/10.1097/rli.0b013e3182087b03
65. Wu X, Kellokumpu-Lehtinen P, Pertovaara H et al (2011) Diffusion-weighted MRI in early chemotherapy response evaluation of patients with diffuse large B-cell lymphoma—a pilot study: comparison with 2-deoxy-2-fluoro-D-glucose-positron emission tomography/computed tomography. NMR Biomed 24:1181–1190. https://doi.org/10.1002/nbm.1689

66. Veronesi U, Cascinelli N, Mariani L et al (2002) Twenty-year follow-up of a randomized study comparing breast-conserving surgery with radical mastectomy for early breast cancer. N Engl J Med 347:1227–1232. https://doi.org/10.1056/nejmoa020989
67. American Cancer Society (2018) Breast cancer survival rate & statistics. https://www.cancer.org/cancer/breast-cancer/understanding-a-breast-cancer-diagnosis/breast-cancer-survival-rates.html. Accessed 7 July 2018
68. Kwast ABG, Groothuis-Oudshoorn KCGM, Grandjean I et al (2012) Histological type is not an independent prognostic factor for the risk pattern of breast cancer recurrences. Breast Cancer Res Treat 135:271–280. https://doi.org/10.1007/s10549-012-2160-z
69. Costelloe CM, Chuang HH, Madewell JE, Ueno NT (2010) Cancer response criteria and bone metastases: RECIST 1.1, MDA and PERCIST. J Cancer. https://doi.org/10.7150/jca.1.80
70. Yang H-L, Liu T, Wang X-M et al (2011) Diagnosis of bone metastases: a meta-analysis comparing 18FDG PET, CT, MRI and bone scintigraphy. Eur Radiol 21:2604–2617. https://doi.org/10.1007/s00330-011-2221-4
71. Zugni F, Ruju F, Pricolo P, Alessi S, Iorfida M, Colleoni MA, Bellomi M, Petralia G (2018) The added value of whole-body magnetic resonance imaging in the management of patients with advanced breast cancer. PLoS ONE 13:e0205251. https://doi.org/10.1371/journal.pone.0205251
72. Peccatori FA, Codacci-Pisanelli G, Del Grande M et al (2017) Whole body MRI for systemic staging of breast cancer in pregnant women. The Breast 35:177–181. https://doi.org/10.1016/j.breast.2017.07.014
73. Goldstein NS (2002) Does the level of E-cadherin expression correlate with the primary breast carcinoma infiltration pattern and type of systemic metastases? Am J Clin Pathol 118:425–434. https://doi.org/10.1309/jmrd-w08y-6k8m-7ad8
74. Usuda K, Sagawa M, Sumiko M et al (2016) Diagnostic performance of whole-body diffusion-weighted imaging compared to PET-CT plus brain MRI in staging clinically resectable lung cancer. Asian Pac J Cancer Prev 17:2775–2780
75. Ohno Y, Yoshikawa T, Kishida Y et al (2017) Diagnostic performance of different imaging modalities in the assessment of distant metastasis and local recurrence of tumor in patients with non-small cell lung cancer. J Magn Reson Imaging 46:1707–1717. https://doi.org/10.1002/jmri.25726
76. Michielsen K, Dresen R, Vanslembrouck R et al (2017) Diagnostic value of whole body diffusion-weighted MRI compared to computed tomography for pre-operative assessment of patients suspected for ovarian cancer. Eur J Cancer 83:88–98. https://doi.org/10.1016/j.ejca.2017.06.010
77. Gorelik N, Reddy SMV, Turcotte RE et al (2017) Early detection of metastases using whole-body MRI for initial staging and routine follow-up of myxoid liposarcoma. Skelet Radiol 47:369–379. https://doi.org/10.1007/s00256-017-2845-9
78. Li FP (1969) Soft-tissue sarcomas, breast cancer, and other neoplasms. Ann Intern Med 71:747–752. https://doi.org/10.7326/0003-4819-71-4-747
79. Mai PL, Best AF, Peters JA et al (2016) Risks of first and subsequent cancers amongTP53mutation carriers in the National Cancer Institute Li–Fraumeni syndrome cohort. Cancer 122:3673–3681. https://doi.org/10.1002/cncr.30248
80. Bojadzieva J, Amini B, Day SF et al (2017) Whole body magnetic resonance imaging (WB-MRI) and brain MRI baseline surveillance in TP53 germline mutation carriers: experience from the Li–Fraumeni Syndrome Education and Early Detection (LEAD) clinic. Fam Cancer 17:287–294. https://doi.org/10.1007/s10689-017-0034-6
81. Saya S, Killick E, Thomas S et al (2017) Baseline results from the UK SIGNIFY study: a whole-body MRI screening study in TP53 mutation carriers and matched controls. Fam Cancer 16:433–440. https://doi.org/10.1007/s10689-017-9965-1
82. Mai PL, Khincha PP, Loud JT et al (2017) Prevalence of cancer at baseline screening in the National Cancer Institute Li–Fraumeni syndrome cohort. JAMA Oncol 3:1640–1645. https://doi.org/10.1001/jamaoncol.2017.1350
83. Villani A, Shore A, Wasserman JD et al (2016) Biochemical and imaging surveillance in germline TP53 mutation carriers with Li–Fraumeni syndrome: 11 year follow-up of a prospective observational study. Lancet Oncol 17:1295–1305. https://doi.org/10.1016/s1470-2045(16)30249-2
84. Anupindi SA, Bedoya MA, Lindell RB et al (2015) Diagnostic performance of whole-body MRI as a tool for cancer screening in children with genetic cancer-predisposing conditions. Am J Roentgenol 205:400–408. https://doi.org/10.2214/ajr.14.13663
85. National Comprehesive Cancer Network (2018) NCCN clinical practice guidelines in oncology (NCCN Guidelines®) for genetic/familial high-risk assessment: breast and ovarian. Version 1
86. Kratz CP, Achatz MI, Brugières L et al (2017) Cancer screening recommendations for individuals with Li–Fraumeni syndrome. Clin Cancer Res 23:e38–e45. https://doi.org/10.1158/1078-0432.ccr-17-0408
87. Else T, Greenberg S, Fishbein L (2018) Hereditary paraganglioma–pheochromocytoma syndromes. https://www.ncbi.nlm.nih.gov/books/NBK1548/. Accessed 5 Oct 2018
88. Rednam SP, Erez A, Druker H et al (2017) Von Hippel–Lindau and hereditary pheochromocytoma/paraganglioma syndromes: clinical features, genetics, and surveillance recommendations in childhood. Clin Cancer Res 23:e68–e75. https://doi.org/10.1158/1078-0432.ccr-17-0547
89. Widemann BC, Blakeley JO, Dombi E et al (2013) Conclusions and future directions for the REiNS International Collaboration. Neurology 81:S41–S44. https://doi.org/10.1212/01.wnl.0000435748.79908.c5
90. Kim JJ, Rini BI, Hansel DE (2010) Von Hippel Lindau syndrome. Adv Exp Med Biol. https://doi.org/10.1007/978-1-4419-6448-9_22
91. Hegenscheid K, Seipel R, Schmidt CO et al (2013) Potentially relevant incidental findings on research whole-body MRI in the general adult population: frequencies and management. Eur Radiol 23:816–826. https://doi.org/10.1007/s00330-012-2636-6
92. Goehde SC, Hunold P, Vogt FM et al (2005) Full-body cardiovascular and tumor MRI for early detection of disease: feasibility and initial experience in 298 subjects. Am J Roentgenol 184:598–611. https://doi.org/10.2214/ajr.184.2.01840598
93. Ulus S, Suleyman E, Aksoy Ozcan U, Karaarslan E (2016) Whole-body MRI screening in asymptomatic subjects; preliminary experience and long-term follow-up findings. Polish J Radiol 81:407–414. https://doi.org/10.12659/pjr.897570
94. Tarnoki DL, Tarnoki AD, Richter A et al (2015) Clinical value of whole-body magnetic resonance imaging in health screening of general adult population. Radiol Oncol 49:10–16. https://doi.org/10.2478/raon-2014-0031
95. Lo GG, Ai V, Au-Yeung KM et al (2008) Magnetic resonance whole body imaging at 3 Tesla: feasibility and findings in a cohort of asymptomatic medical doctors. Hong Kong Med J Xianggang yi xue za zhi 14:90–96
96. Cieszanowski A, Maj E, Kulisiewicz P et al (2014) Non-contrast-enhanced whole-body magnetic resonance imaging in the general population: the incidence of abnormal findings in patients 50 years old and younger compared to older subjects. PLoS ONE 9:e107840. https://doi.org/10.1371/journal.pone.0107840
97. Bamberg F, Kauczor H-U, Weckbach S et al (2015) Whole-body MR imaging in the German National Cohort: rationale, design, and technical background. Radiology 277:206–220. https://doi.org/10.1148/radiol.2015142272

98. UK Biobank (2018) UK Biobank—UK Biobank MRI Imaging Study. http://www.ukbiobank.ac.uk/scanning-study-launches/. Accessed 7 July 2018
99. Ollivier L (2006) Improving the interpretation of bone marrow imaging in cancer patients. Cancer Imaging 6:194–198. https://doi.org/10.1102/1470-7330.2006.0034
100. Padhani AR (2014) Whole-body MRI and diffusion MRI. Cancer Imaging 14:O31. https://doi.org/10.1186/1470-7330-14-S1-O31
101. Koh D-M, Blackledge M, Padhani AR et al (2012) Whole-body diffusion-weighted MRI: tips, tricks, and pitfalls. Am J Roentgenol 199:252–262. https://doi.org/10.2214/AJR.11.7866
102. Padhani AR, Makris A, Gall P et al (2014) Therapy monitoring of skeletal metastases with whole-body diffusion MRI. J Magn Reson Imaging 39:1049–1078. https://doi.org/10.1002/jmri.24548
103. Padhani AR, Gogbashian A (2011) Bony metastases: assessing response to therapy with whole-body diffusion MRI. Cancer Imaging 11:S1–S17. https://doi.org/10.1102/1470-7330.2011.9034